Metal–Metal-Bonded Compounds of Lower-Valent Niobium and Tantalum. Compounds Containing the $[Nb_2Cl_7(PR_3)_2]^-$ and $[Nb_3Cl_{10}(PR_3)_3]^-$ Ions and Some Clues As to How Higher-Nuclearity Clusters Are Formed

F. Albert Cotton* and Maoyu Shang

Department of Chemistry and Laboratory for Molecular Structure and Bonding, Texas A&M University, College Station, Texas 77843

Received October 1, 1992

Two examples of a new type of face-sharing bioctahedral diniobium cluster that contain three bridging chloride ligands and two terminal phosphines in a syn configuration, $(Bu_4N)[Nb_2Cl_7(PEt_3)_2]$ (**1**) and $(Bu_4N)[Nb_2Cl_7(PMe_3)_2]\cdot THF$ (**2**), as well as a related triangular trinuclear niobium cluster, $(HPMe_3)(Bu_4N)[Nb_3Cl_{10}(PMe_3)_3](BF_4)\cdot THF$ (**3**), have been synthesized and characterized by X-ray diffraction. Complex **1** crystallizes in the space group $R\bar{3}c$, with $a = b = 32.265(3)$ Å, $c = 25.579(3)$ Å, $V = 23061(8)$ Å^3, and $Z = 18$; Nb–Nb distance = 2.708(3) Å. Compound **2** belongs to the space group $P2_1$, with $a = 10.177(4)$ Å, $b = 19.602(3)$ Å, $c = 10.557(3)$ Å, $\beta = 90.38(3)°$, $V = 2105(1)$ Å^3, and $Z = 2$; Nb–Nb distance = 2.683(1) Å. The trinuclear cluster **3** crystallizes in the space group $R\bar{3}$, with $a = b = 40.595(5)$ Å, $c = 19.253(4)$ Å, $V = 27477(8)$ Å^3, and $Z = 18$; average Nb–Nb distance = 2.959[12] Å (2.974(3), 2.944(3), and 2.958(3) Å). Compounds **1** and **2** have effective magnetic moments 0.84 and 0.99 μ_B at room temperature, respectively. A conversion from $[Nb_2Cl_7(PEt_3)_2]^-$ to $[Nb_3Cl_{10}(PEt_3)_3]^-$ has been observed and is discussed. Pathways of conversion from edge-sharing bioctahedral $Nb_2Cl_6(PEt_3)_4$ to the face-sharing $[Nb_2Cl_7(PEt_3)_2]^-$ and finally to triangular trinuclear $[Nb_3Cl_{10}(PEt_3)_3]^-$ or even larger clusters are discussed.

Introduction

In recent years much effort has been devoted in this laboratory to exploring the chemistry of di-, tri-, and tetranuclear compounds of niobium and tantalum in formal oxidation states in the range of +2 to +4. It is a common characteristic of all these compounds, structurally diverse though they are, that the metal atoms employ all d electrons to form M–M bonds. The bond orders range from 1 to 3.[1-10]

Our principal efforts have been devoted to the major subset of these compounds that contain only metal atoms, chlorine atoms and phosphine molecules. Within this subset the structural types have been (1) many edge-sharing bioctahedral species,[11-19] nearly all of which contain bridging or chelating biphosphines (the only reported example in which there are monophosphines appears to be $Ta_2Cl_6(PMe_3)_4$[19]), (2) numerous trinuclear species[1,2] of the general type $M_3(\mu_3\text{-}Cl)(\mu\text{-}Cl)_3Cl_n(PR_3)_{9-n}$, and (3) some tetranuclear clusters that consist of two of the preceding trinuclear units fused on a common edge.[3] There have not been any prior reports of face-sharing bioctahedral species of this subset (i.e., containing three M–Cl atoms and a mixture of Cl and PR_3 ligands making up the set of six terminal ligands) although the $[Nb_2Cl_9]^{3-}$ ion and numerous species with bridging ligands other than Cl are known.

The several trinuclear and tetranuclear species are well understood from the point of view of structure and bonding but not with regard to how they are formed. In the course of work carried out to develop some understanding of how the larger clusters arise, we have been fortunate enough to prepare and characterize the first face-sharing bioctahedral diniobium species containing only chloride atoms and phosphine molecules. The two purposes of this paper are to describe these compounds and to discuss how they may help to understand the process by which the larger niobium cluster species that contain only the same components are formed.

Experimental Section

All manipulations were carried out under an atmosphere of argon, usually by employing standard Schlenk techniques. Solvents, tetrahydrofuran, ether, and hexane were distilled over Na–K alloy/benzophenone, and dichloromethane was distilled over phosphorus pentoxide. Visible spectra were recorded on a Cary 17D spectrophotometer. Infrared spectra in the range 4000–200 cm^{-1} were measured on a Perkin-Elmer 783 infrared spectrophotometer. Magnetic susceptibility data were obtained on a Johnson Matthey magnetic susceptibility balance at 26 °C. Elemental analyses were performed by Galbraith Laboratories Inc., Knoxville, TN. Magnesium turnings, anhydrous $MgCl_2$, trimethylphosphine and triethylphosphine were purchased from Aldrich Co. Tetrabutylammonium tetrafluoroborate (Bu_4NBF_4) was obtained from Strem Chemicals Inc. and dried at 80 °C on a vacuum line for 6 h. The $MgCl_2$ was recrystallized

(1) Cotton, F. A.; Diebold, M. P.; Feng, X.; Roth, W. J. *Inorg. Chem.* **1988**, *27*, 3413.
(2) Cotton, F. A.; Babaian-Kibala, E.; Shang, M. *Inorg. Chem.* **1990**, *29*, 5148.
(3) (a) Cotton, F. A., Shang, M. *J. Am. Chem. Soc.* **1988**, *23*, 7719. (b) Babaian-Kibala, E.; Cotton, F. A. *Acta Crystallogr.* **1991**, *C47*, 1716.
(4) Cotton, F. A.; Shang, M. *Organometallics* **1990**, *9*, 2131 and earlier references therein.
(5) Babaian-Kibala, E.; Cotton, F. A.; Kibala, P. A. *Polyhedron* **1990**, *9*, 1689.
(6) Cotton, F. A.; Babaian-Kibala, E.; Falvello, L. R.; Shang, M. *Inorg. Chem.* **1990**, *29*, 2591.
(7) Cotton, F. A.; Babaian-Kibala, E.; Shang, M. *Acta Crystallogr.* **1991**, *C47*, 1617.
(8) Babaian-Kibala, E.; Cotton, F. A.; Kibala, P. A. *Inorg. Chem.* **1990**, *29*, 4002.
(9) Babaian-Kibala, E.; Cotton, F. A. *Inorg. Chim. Acta* **1990**, *171*, 71.
(10) Messerle, L. *Chem. Rev.* **1988**, *88*, 1229.
(11) Canich, J. A. M.; Cotton, F. A. *Inorg. Chem.* **1987**, *26*, 4236.
(12) Cotton, F. A.; Diebold, M. P.; Roth, W. J. *Inorg. Chem.* **1987**, *26*, 4130.
(13) Cotton, F. A.; Roth, W. J. *Inorg. Chim. Acta* **1983**, *71*, 175.
(14) Cotton, F. A.; Falvello, L. R.; Najjar, R. *Inorg. Chem.* **1983**, *22*, 375.
(15) Cotton, F. A.; Roth, W. J. *Inorg. Chem.* **1983**, *22*, 3654.
(16) Cotton, F. A.; Duraj, S. A.; Falvello, L. R.; Roth, W. J. *Inorg. Chem.* **1985**, *24*, 4389.
(17) Chakravarty, A. R.; Cotton, F. A.; Diebold, M. P.; Lewis, D. B.; Roth, W. J. *J. Am. Chem. Soc.* **1986**, *108*, 971.
(18) Ferm, B.; Johnson, T.; Francis, S.; Messerle, L. *Abstracts of Papers*, 195th National Meeting of the American Chemical Society, Toronto; American Chemical Society: Washington, DC, 1988; No. 589.
(19) Sattelberger, A. P.; Wilson, R. B., Jr.; Huffman, J. C. *Inorg. Chem.* **1982**, *21*, 2392.

0020-1669/93/1332-0969$04.00/0

Table I. Crystallographic Data for $(Bu_4N)[Nb_2Cl_7(PEt_3)_2]$ (**1**), $(Bu_4N)[Nb_2Cl_7(PMe_3)_2]\cdot THF$ (**2**), and $(HPMe_3)(Bu_4N)[Nb_3Cl_{10}(PMe_3)_3](BF_4)\cdot THF$ (**3**)

	1	**2**	**3**
formula	$Nb_2Cl_7P_2NC_{28}H_{66}$	$Nb_2Cl_7P_2ONC_{26}H_{62}$	$Nb_3Cl_{10}P_4F_4ONC_{32}BH_{81}$
fw	912.27	900.72	1339.96
space group	$R\bar{3}c$	$P2_1$	$R\bar{3}$
a, Å	32.265(5)	10.177(4)	40.596(5)
b, Å	32.265(5)	19.602(3)	40.595(5)
c, Å	25.579(3)	10.557(3)	19.253(4)
α, deg	90.0	90.0	90.0
β, deg	90.0	90.38(3)	90.0
γ, deg	120.0	90.0	120.0
V, Å^3	23061(8)	2105(1)	27477(8)
Z	18	2	18
d_{calcd}, g/cm^3	1.183	1.420	1.458
λ, Å	0.710 73	0.710 73	0.710 73
μ, cm^{-1}	8.741	10.636	11.117
T, °C	20	−40	20
transm coeff	0.9744–0.9069	0.9984–0.8686	0.9938–0.9472
$R(F_o)^a$	0.060	0.047	0.062
$R_w(F_o)^b$	0.082	0.064	0.100

^{a} $R(F_o) = \sum||F_o| - |F_c||/|F_o|$. ^{b} $R_w(F_o) = [\sum w(|F_o| - |F_c|)^2/\sum w|F_o|^2]^{1/2}$.

from an ether/hexane (1:1) mixture and dried on a vacuum line at 120 °C for 6 h. $NbCl_4(THF)_2$ was prepared according to the literature method.[20]

Synthesis of $(Bu_4N)[Nb_2Cl_7(PEt_3)_2]$ (1). $NbCl_4(THF)_2$ (3.79 g, 10 mmol), Mg turnings (125 mg, 5.14 mmol), Bu_4NBF_4 (1.65 g, 5.01 mmol) and PEt_3 (1.5 mL, 10.28 mmol) were stirred in 50 mL of THF in a 250 mL three-necked flask. Yellow $NbCl_4(THF)_2$ reacted rapidly with PEt_3 to form a brown solution. The magnesium turnings were fully dissolved in about 6 h to yield an emerald solution. After another 24 h of reaction time the solution had turned blue-green. Hexane (30 mL) was then carefully added on the surface of the solution and the flask was kept in a refrigerator at 0 °C for 3 days. Green needle-like crystals (longer than 1 cm) were collected by filtration. Yield: 2.8 g. Another portion of hexane (30 mL) was added to the brown-green filtrate and the solution was kept at 0 °C for another 3 days to yield another crop of green crystals. Yield: ca. 0.86 g. The combined yield is ca. 80%. A pure sample was obtained by recrystallization from a THF/hexane mixture (1:1) or a CH_2Cl_2/hexane mixture (1:1.5). Yield: ca. 2.5 g, 55%. Anal. Calcd C, 36.84; H, 7.29; N, 1.53; P, 6.79; Cl, 27.19. Found (first crop): C, 33.84; H, 6.75; N, 1.34; P, 4.70; Cl, 36.89. Found (recrystallized product): C, 35.34; H, 7.21; N, 1.29; P, 5.73; Cl, 26.58. IR (Nujol, CsI plates, cm^{-1}) for the purified product: 1483 w, 1425 w, 1266 m, 1151 m, 1043 s, 84 m, 759 s, 736 w, 671 w, 625 w, 345 w, 326 w, 311 s. Visible spectrum in THF: 637 nm, ϵ_{max} 3300 M^{-1} cm^{-1}.

Synthesis of $(Bu_4N)[Nb_2Cl_7(PMe_3)_2]\cdot THF$ (2) and $(HPMe_3)(Bu_4N)[Nb_3Cl_{10}(PMe_3)_3](BF_4)\cdot THF$ (3). $NbCl_4(THF)_2$ (0.76 g, 2 mmol), Mg turnings (25 mg, 1.1 mmol), Bu_4NBF_4 (0.33 g, 1 mmol), and PMe_3 (0.3 mL, 3.0 mmol) were stirred in 40 mL of THF. The Mg turnings dissolved in about 8 h and a mixture of a green-blue crystalline precipitate and a green solution was formed. After a total of 24 h of stirring, the reaction mixture was filtered, and the green-blue crystalline precipitate was washed with THF. Yield: 0.66 g, 73%. Anal. Calcd for **2**: C, 34.67; H, 6.94; N, 1.56; P, 6.88; Cl, 27.55. Found: C, 32.95; H, 6.94; N, 1.45; P, 6.67; Cl, 26.01. Visible absorption in THF: 630 nm, ϵ_{max} 3100 M^{-1} cm^{-1}. The brownish green filtrate was layered with hexane (40 mL) in a Schlenk tube. Along with a white precipitate and a brown oily substance, another crop of green crystals (ca. 50 mg, 6.5%) and well-formed brown crystals were formed in 2 weeks. The brown crystals were later characterized by X-ray diffraction to be **3**. Yield: ca. 150 mg, 11%.

X-ray Crystallography of $(Bu_4N)[Nb_2Cl_7(PEt_3)_2]$ (1). Crystals were examined in a stream of argon under a mixture of mineral oil and mother liquor (4:1), wedged in capillaries filled with argon, and sealed by flame for crystallography. Unit cell parameters were obtained by centering and indexing 25 reflections that were found by rotation photography, and refined by centering another 25 reflections in the range $27° < 2\theta < 30°$ that were obtained by preliminary data collection. The Laue class $\bar{3}m$ and axial dimensions were confirmed by axial photography. Three intensity and orientation standards were checked after every 97 intensity measurements, which showed no obvious change of the crystal orientation, but a total of 11.6% decay during the data collection. The intensity data were corrected for Lorentz and polarization effects,[21] anisotropic decay and an empirical absorption correction based on azimuthal scans of seven reflections with their χ angles near 90°. The R_{int} for averaging equivalent intensity data was 0.035. On the basis of the systematic absences, the possible space groups were $R3c$ and $R\bar{3}c$. Successful solution and refinement of the structure confirmed the latter.

The positional parameters of the Nb atoms and Cl atoms were provided by the Patterson method.[22] The ensuing combination of difference Fourier syntheses and least-squares refinements revealed all remaining non-hydrogen atoms and revealed that two terminal carbon atoms of the ammonium cation, C(10) and C(14), were disordered, with each one on two positions. Since electron densities for each pair of positions on a difference Fourier map were close, in the final refinement all these positions were assigned site occupancies of 0.5, and the atoms were treated isotropically, but all the other atoms were refined anisotropically. The final difference Fourier map was featureless with a highest peak height of 0.188 e/Å^3. The crystallographic data are listed in Table I. Atomic positional and thermal parameters are shown in Table II. Some important bond distances and angles are listed in Table III.

Table II. Positional and Equivalent Isotropic Thermal Parameters for $(Bu_4N)[Nb_2Cl_7(PEt_3)_2]$

atom	x	y	z	B,^{a} Å^2
Nb	0.55763(5)	0.51458(5)	0.27427(6)	5.49(4)
Cl(1)	0.6021(2)	0.6021(2)	0.250	6.9(1)
Cl(2)	0.5068(2)	0.4804(1)	0.1954(2)	9.0(1)
Cl(3)	0.5919(2)	0.5392(2)	0.3599(2)	9.4(2)
Cl(4)	0.6226(1)	0.5098(2)	0.2345(2)	7.5(1)
P	0.5253(2)	0.4265(2)	0.3056(3)	10.5(2)
C(1)	0.472(1)	0.3973(8)	0.343(1)	19(1)
C(2)	0.480(1)	0.4219(9)	0.392(1)	22(1)
C(3)	0.4994(9)	0.3793(6)	0.255(1)	19(1)
C(4)	0.526(1)	0.3763(9)	0.226(1)	20(1)
C(5)	0.5754(7)	0.4247(6)	0.341(1)	13.3(8)
C(6)	0.565(1)	0.3766(9)	0.361(1)	21(1)
N	0.7469(7)	0.7469(7)	0.750	8.8(5)
C(7)	0.7512(7)	0.7955(6)	0.7401(8)	10.7(7)
C(8)	0.7745(9)	0.8268(6)	0.787(1)	15.9(9)
C(9)	0.777(2)	0.870(1)	0.770(1)	26(2)
C(10)	0.815(2)	0.917(2)	0.798(3)	22(3)*
C(10)′	0.755(3)	0.884(3)	0.803(3)	25(3)*
C(11)	0.7234(6)	0.7201(6)	0.6988(7)	8.8(6)
C(12)	0.7150(9)	0.6702(7)	0.7015(7)	13.2(9)
C(13)	0.683(1)	0.6420(7)	0.6566(9)	19(1)
C(14)	0.662(2)	0.592(2)	0.661(2)	14(2)*
C(14)′	0.700(3)	0.605(3)	0.653(3)	25(3)*

^{a} Starred values indicate that atoms were refined isotropically. Anisotropically refined atoms are given in the form of the equivalent isotropic displacement parameter defined as $(4/3)[a^2\beta_{11} + b^2\beta_{22} + c^2\beta_{33} + ab(\cos\gamma)\beta_{12} + ac(\cos\beta)\beta_{13} + bc(\cos\alpha)\beta_{23}]$.

X-ray Crystallography of $(Bu_4N)[Nb_2Cl_7(PMe_3)_2]\cdot THF$ (2). Crystals were handled under a layer of a mineral oil/mother liquor (4:1) mixture in an atmosphere of argon, mounted on the top of glass fibers with the Apiezon T grease, and transferred to goniometer heads under a cold stream of N_2 (−60 °C) for X-ray crystallography. Cell parameters were obtained by centering and indexing 25 randomly found reflections, refined by centering 25 reflections in the range $24° < 2\theta < 27°$, and confirmed by axial photography, along with the Laue class $2/m$. A learned profile analysis[23] was used to increase the $I/\sigma(I)$ values for reflections with values less than 25. No obvious crystal decay nor crystal dislocation was observed during the data collection by monitoring three standard reflections. Systematic absences showed two possible space groups $P2_1$ and $P2_1/m$. However, the latter was ruled out by the absence of significant peaks located on the Harker line $(0, y, 0)$ (absence of the mirror plane) in a three-dimensional Patterson map.

The positions of the two independent metal atoms were derived from a Patterson map, assuming the $P2_1$ space group. A following series of least-squares refinements and difference Fourier syntheses successfully revealed all the other nonhydrogen atoms. In the interstitial THF ring,

(20) Manzer, L. *Inorg. Chem.* **1977**, *16*, 525.

(21) Calculations were done on a local Area VAX Cluster (VMS X4.6) with the commercial package SDP/VV3.0.

(22) Sheldrick, G. M. SHELXS-86, Program for X-ray Crystal Structure Determination. University of Gottingen, Germany, 1986.

(23) *CAD4 User's Manual*; Enraf-Nonius, Delft Scientific Instruments Division: Delft, The Netherlands, 1988.

Table III. Important Bond Distances (Å) and Angles (deg) for $(Bu_4N)[Nb_2Cl_7(PEt_3)_2]$[a]

Distances			
Nb–Nb′	2.708(3)	Nb–Cl(2)′	2.500(5)
Nb–Cl(1)	2.524(5)	Nb–Cl(3)	2.403(5)
Nb′–Cl(1)	2.524(5)	Nb–Cl(4)	2.403(5)
Nb–Cl(2)	2.482(5)	Nb–P	2.617(6)
Angles			
Cl(1)–Nb–Cl(2)	100.2(1)	Cl(2)′–Nb–Cl(3)	91.2(2)
Cl(1)–Nb–Cl(2)′	99.7(2)	Cl(2)′–Nb–Cl(4)	169.3(2)
Cl(1)–Nb–Cl(3)	86.8(1)	Cl(2)′–Nb–P	87.8(2)
Cl(1)–Nb–Cl(4)	86.7(2)	Cl(3)–Nb–Cl(4)	97.8(2)
Cl(1)–Nb–P	170.4(2)	Cl(3)–Nb–P	87.0(2)
Cl(2)–Nb–Cl(2)′	78.7(2)	Cl(4)–Nb–P	86.9(2)
Cl(2)–Nb–Cl(3)	168.5(2)	Nb–Cl(1)–Nb′	64.87(8)
Cl(2)–Nb–Cl(4)	91.8(2)	Nb–Cl(2)–Nb′	65.8(1)
Cl(2)–Nb–P	87.2(2)		

[a] Numbers in parentheses are estimated standard deviations in the least significant digits.

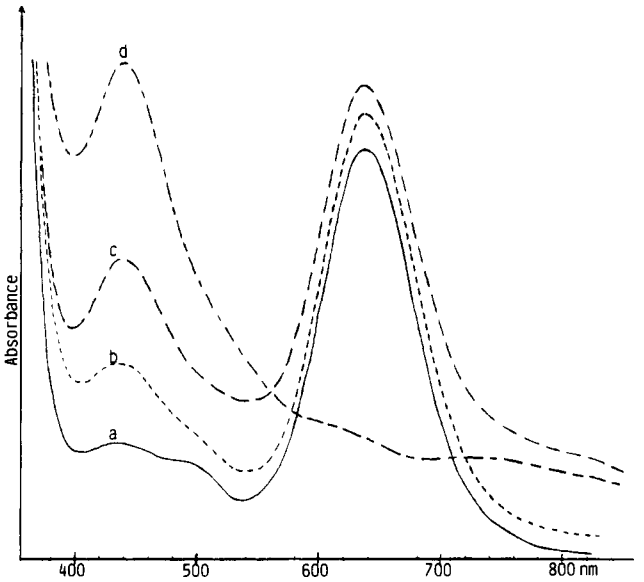

Figure 1. Visible spectra of the reaction system of $NbCl_4(THF)_2$–Mg–PEt_3 in THF: (a) after 7 h (—); (b) after 13 h (- - -); (c) after 3 days (– – –); (d) after 7 days (– · – · –).

the oxygen atom was assigned to the ring atom that had the smallest isotropic thermal parameter after all these ring atoms were refined isotropically as carbon atoms. In the final least-squares refinement all these atoms were treated anisotropically. The first several peaks in the final difference Fourier map were all in the vicinity of the heavy atoms. The enantiomeric structure was also tried. However, the refinement converged to higher values for R and R_w values (0.052 and 0.073, respectively) and for the goodness of fit indicator (2.176), which was indicative of the correctness of the former choice.

The crystallographic data are shown in Table I. The positional and thermal parameters are listed in Table IV. Selected bond distances and angles are listed in Table V.

X-ray Crystallography of $(HPMe_3)(Bu_4N)[Nb_3Cl_{10}(PMe_3)_3](BF_4)\cdot THF$ (3). Crystal handling and X-ray crystallography were essentially the same as those of **1** except that the 25 reflections that were used to refine the unit cell parameters came from the shell $26° < 2\theta < 28°$ as diffraction from the crystal was a little weaker than in the former case. The overall decay of the crystal was 24.7% during the data collection. Therefore, the corresponding anisotropic decay correction was applied along with the routine Lp and absorption corrections. The averaging of the equivalent intensity data then yielded 0.035 for the agreement factor R_{int}. The Laue class $\bar{3}$ was supported by axial photography and by checking possible equivalent reflections. Except for the intrinsic systematic absences $-h + k + l \neq 3n$ for all reflections that were created by transformation from a primitive rhombohedral cell to a hexagonal cell, no other systematic absences were observed, which narrowed the possible space groups to $R3$ and $R\bar{3}$.

Table IV. Positional and Equivalent Isotropic Thermal Parameters for $(Bu_4N)[Nb_2Cl_7(PMe_3)_2]\cdot THF$

atom	x	y	z	B,[a] Å^2
Nb(1)	0.4465(1)	0.500	0.4933(1)	2.73(2)
Nb(2)	0.6561(1)	0.58303(7)	0.4969(1)	2.59(2)
Cl(1)	0.6264(3)	0.4890(2)	0.6521(3)	3.23(6)
Cl(2)	0.6429(3)	0.4806(2)	0.3575(3)	3.39(7)
Cl(3)	0.4231(4)	0.6282(2)	0.4743(5)	6.1(1)
Cl(4)	0.3032(3)	0.4920(2)	0.3138(3)	4.91(8)
Cl(5)	0.2895(3)	0.5027(2)	0.6646(3)	4.36(7)
P(1)	0.4236(4)	0.3693(2)	0.5049(4)	3.53(8)
Cl(6)	0.7134(4)	0.6547(2)	0.3213(3)	4.73(8)
Cl(7)	0.6893(4)	0.6653(2)	0.6627(3)	4.26(8)
P(2)	0.9027(3)	0.5563(2)	0.5329(4)	3.65(8)
C(1)	0.256(2)	0.341(1)	0.487(2)	7.5(5)
C(2)	0.479(3)	0.328(1)	0.648(2)	9.0(6)
C(3)	0.510(2)	0.321(1)	0.387(2)	8.6(5)
C(4)	0.965(1)	0.4796(8)	0.464(2)	4.9(4)
C(5)	1.012(1)	0.6221(8)	0.480(2)	4.6(3)
C(6)	0.946(1)	0.550(1)	0.700(1)	5.5(4)
N	0.401(1)	0.6458(6)	0.972(1)	3.9(3)
C(7)	0.487(1)	0.5799(9)	0.936(1)	4.6(3)
C(8)	0.559(2)	0.553(1)	1.051(1)	5.1(4)
C(9)	0.630(2)	0.4848(9)	1.006(1)	4.8(4)
C(10)	0.539(2)	0.428(1)	0.988(2)	7.1(5)
C(11)	0.479(2)	0.6994(8)	1.034(1)	4.7(4)
C(12)	0.599(2)	0.725(1)	0.961(1)	6.0(4)
C(13)	0.677(2)	0.779(1)	1.031(2)	7.2(5)
C(14)	0.774(2)	0.813(2)	0.962(3)	13.0(8)
C(15)	0.346(2)	0.6688(9)	0.840(1)	4.7(3)
C(16)	0.264(2)	0.7334(9)	0.853(1)	5.4(4)
C(17)	0.181(2)	0.741(1)	0.733(1)	5.6(4)
C(18)	0.112(2)	0.812(1)	0.731(2)	7.8(5)
C(19)	0.291(1)	0.6266(9)	1.062(1)	4.5(3)
C(20)	0.203(1)	0.568(1)	1.014(1)	5.4(4)
C(21)	0.077(2)	0.571(1)	1.094(2)	7.2(5)
C(22)	−0.003(3)	0.508(3)	1.069(2)	20(2)
O	0.787(2)	0.2864(8)	0.826(1)	8.8(4)
C(23)	0.865(2)	0.346(1)	0.846(2)	9.2(6)
C(24)	0.986(2)	0.342(1)	0.752(2)	10.0(7)
C(25)	0.926(3)	0.301(1)	0.656(3)	14.7(9)
C(26)	0.822(2)	0.253(1)	0.714(2)	8.0(6)

[a] Anisotropically refined atoms are given in the form of the equivalent isotropic displacement parameter defined as $(4/3)[a^2\beta_{11} + b^2\beta_{22} + c^2\beta_{33} + ab(\cos\gamma)\beta_{12} + ac(\cos\beta)\beta_{13} + bc(\cos\alpha)\beta_{23}]$.

Direct methods[22] provided the positions of the three independent Nb atoms in the $R\bar{3}$ space group. Ensuing least-squares refinements and difference Fourier syntheses gradually revealed the title compound, a very unusual combination of four types of ions and a solvent. While the niobium trimer anion was ordered, all the other three ions were found to be disordered in different ways. In the tetrabutylammonium group, a butyl chain extended in two directions from the γ carbon atom (C(24) and C(25), and C(24)′ and C(25)′). The tetrafluoroborate group is found in two orientations with one tetrahedral set of F atoms rotated around the central boron atom away from the other set by about 46°. The trimethylphosphine group was completely disordered on two sets of general positions in such a way that a PC_3 tripod could be regarded as entangled with its mirror image which is slid along the mirror to make a slight separation between the two sets of C_3 atoms. Before the final refinement an oxygen atom was assigned to a five-membered ring atom in the same way as that of the THF molecule in **2**. In the final refinement all the above disordered atoms and the solvent molecule were refined with isotropic thermal parameters and bond distance constraints (C–C and C–O, 1.540 Å, B–F, 1.380 Å, P–C, 1.800 Å).[24]

The site occupancies for the above three sets of disordered atoms converged eventually to 0.66(7)/0.34(7), 0.50(4)/0.50(4), and 0.55(3)/0.45(3), respectively. The final difference Fourier map was then nearly featureless with remaining peaks too low to make chemical sense. The crystallographic data are compiled in Table I. The positional and thermal parameters are listed in Table VI. Some important bond parameters are listed in Table VII. ORTEP drawings for these disordered ions have been deposited as supplementary material.

(24) Sheldrick, G. M. SHELX-76, Program for X-ray Crystal Structure Determination. University of Cambridge, England, 1976.

Table V. Selected Bond Distances (Å) and Angles (deg) for $(Bu_4N)[Nb_2Cl_7(PMe_3)_2]\cdot THF$[a]

Distances			
Nb(1)–Nb(2)	2.683(1)	Nb(2)–Cl(1)	2.486(3)
Nb(1)–Cl(1)	2.482(3)	Nb(2)–Cl(2)	2.493(3)
Nb(1)–Cl(2)	2.498(3)	Nb(2)–Cl(3)	2.542(4)
Nb(1)–Cl(3)	2.534(4)	Nb(2)–Cl(6)	2.401(4)
Nb(1)–Cl(4)	2.389(4)	Nb(2)–Cl(7)	2.402(4)
Nb(1)–Cl(5)	2.423(3)	Nb(2)–P(2)	2.590(4)
Nb(1)–P(1)	2.577(4)		
Angles			
Cl(1)–Nb(1)–Cl(2)	77.6(1)	Cl(1)–Nb(2)–Cl(6)	166.9(1)
Cl(1)–Nb(1)–Cl(3)	102.0(1)	Cl(1)–Nb(2)–Cl(7)	92.0(1)
Cl(1)–Nb(1)–Cl(4)	166.7(1)	Cl(1)–Nb(2)–P(2)	82.8(1)
Cl(1)–Nb(1)–Cl(5)	89.2(1)	Cl(2)–Nb(2)–Cl(3)	100.3(1)
Cl(1)–Nb(1)–P(1)	87.1(1)	Cl(2)–Nb(2)–Cl(6)	91.6(1)
Cl(2)–Nb(1)–Cl(3)	100.4(1)	Cl(2)–Nb(2)–Cl(7)	167.9(1)
Cl(2)–Nb(1)–Cl(4)	91.2(1)	Cl(2)–Nb(2)–P(2)	88.4(1)
Cl(2)–Nb(1)–Cl(5)	165.3(1)	Cl(3)–Nb(2)–Cl(6)	87.4(2)
Cl(2)–Nb(1)–P(1)	87.1(1)	Cl(3)–Nb(2)–Cl(7)	87.7(2)
Cl(3)–Nb(1)–Cl(4)	86.9(2)	Cl(3)–Nb(2)–P(2)	170.8(2)
Cl(3)–Nb(1)–Cl(5)	88.6(2)	Cl(6)–Nb(2)–Cl(7)	97.8(1)
Cl(3)–Nb(1)–P(1)	169.2(1)	Cl(6)–Nb(2)–P(2)	89.5(1)
Cl(4)–Nb(1)–Cl(5)	101.0(1)	Cl(7)–Nb(2)–P(2)	84.1(1)
Cl(4)–Nb(1)–P(1)	85.2(1)	Nb(1)–Cl(1)–Nb(2)	65.38(8)
Cl(5)–Nb(1)–P(1)	85.8(1)	Nb(1)–Cl(2)–Nb(2)	65.04(8)
Cl(1)–Nb(2)–Cl(2)	77.6(1)	Nb(1)–Cl(3)–Nb(2)	63.8(1)
Cl(1)–Nb(2)–Cl(3)	101.7(1)		

[a] Numbers in parentheses are estimated standard deviations in the least significant digits.

Tracking the Formation of the Trinuclear Cluster. THF solutions of crystalline samples of the known $(HPEt_3)[Nb_3Cl_{10}(PEt_3)_3]$ (**4**) and $[Mg_2Cl_3(THF)_6][Nb_3Cl_{10}(PEt_3)_3]$ (**5**)[2] were first prepared and their visible spectra were recorded. These showed two distinct absorption bands at ~435 nm with ϵ_{max} 2400 M^{-1} cm^{-1} (435 nm for **4** and 434 nm for **5**) and ~745 nm with ϵ_{max} 450 M^{-1} cm^{-1} (743 nm for **4** and 747 nm for **5**).

After 7 h of reduction of $NbCl_4(THF)_2$ (2 mmol) in THF (25 mL) at 26 °C by Mg turnings (1.1 mmol) in the presence of PEt_3 (3 mmol), the Mg turnings had disappeared and an emerald solution had formed. The solution showed a very intense band at 637 nm, similar to that of the THF solution prepared from the recrystallized $(Bu_4N)[Nb_2Cl_7(PEt_3)_2]$, as well as a weak trinuclear band at 435 nm, and an even weaker band at 490 nm (Figure 1a). After 6 h more of stirring the color of the solution changed to dark green. The intensity of the band at 637 nm was somewhat reduced and the band at 490 nm became a barely discernible shoulder, while the trimer band at 435 nm was more intense (Figure 1b). After a total of 3 days of stirring, the solution was brownish green and had become cloudy, or else had deposited a brown precipitate, which did not dissolve in common organic solvents such as THF, benzene, acetonitrile, and ether. The background in the spectrum was raised, the band at 490 nm was gone and the intensity ratio of the trimer/dimer bands had increased (Figure 1c). After a week of reaction, the solution had become brown and much brown precipitate was present. Only the trimer band showed up on a very high background (Figure 1d).

When $MgCl_2$ (1 mmol) or Bu_4NBF_4 (1 mmol) was added to the reaction system, after 60 h of stirring the solution became a mixture of a brown solution and a brown precipitate. When the reaction was carried out at 50 °C, a mixture of brown solution and a brown precipitate was again formed over a period of 2 days.

Results and Discussion

Crystal Structure of $(Bu_4N)[Nb_2Cl_7(PEt_3)_2]$ (1). The crystal consists of tetrabutylammonium cations and diniobium cluster anions, the latter having the configuration shown in Figure 2. It is the first face-sharing bioctahedral diniobium structure containing only halogen bridges to be synthesized by solution chemistry. Apart from the three bridging chlorine atoms each metal atom is further coordinated terminally by two chlorine atoms and one phosphine molecule. There is a crystallographic 2-fold axis going through one bridging chlorine atom (Cl(1)) and the midpoint of the metal–metal bond. However, the cluster core possesses effectively a C_{2v} symmetry. The oxidation state of the metal atoms is +3. The metal–metal distance, 2.708(3) Å, is quite comparable to the metal–metal doubly-bonded distances in other face-sharing bioctahedral diniobium derivatives, 2.696(1)–2.741(3) Å. Although the Nb–P bonds (2.617(6) Å)

Table VI. Positional and Equivalent Isotropic Thermal Parameters for $(HPMe_3)(Bu_4N)[Nb_3Cl_{10}(PMe_3)_3](BF_4)\cdot THF$

atom	*x*	*y*	*z*	B,[a] Å^2
Nb(1)	0.18353(6)	0.07860(6)	0.17025(9)	3.41(7)
Nb(2)	0.18312(6)	0.08133(6)	0.3246(1)	3.72(8)
Nb(3)	0.13752(6)	0.00841(6)	0.2504(1)	3.90(8)
Cl(1)	0.2083(2)	0.0481(2)	0.2517(3)	3.9(2)
Cl(2)	0.1673(2)	0.1180(2)	0.2433(3)	4.3(2)
Cl(3)	0.1144(2)	0.0379(2)	0.3351(3)	4.7(2)
Cl(4)	0.1152(2)	0.0344(2)	0.1598(3)	4.5(2)
Cl(5)	0.1952(2)	0.0471(2)	0.0756(3)	5.4(3)
Cl(6)	0.2478(2)	0.1309(2)	0.1586(3)	4.9(2)
P(1)	0.1710(2)	0.1133(2)	0.0664(3)	5.4(3)
Cl(7)	0.2469(2)	0.1351(2)	0.3338(3)	5.2(2)
Cl(8)	0.1937(2)	0.0525(2)	0.4250(3)	6.5(3)
P(2)	0.1705(2)	0.1198(2)	0.4220(4)	5.8(3)
Cl(9)	0.1418(2)	–0.0303(2)	0.3415(3)	6.7(3)
Cl(10)	0.1438(2)	–0.0327(2)	0.1673(4)	6.1(3)
P(3)	0.0658(2)	–0.0465(2)	0.2504(4)	6.7(3)
C(1)	0.1313(9)	0.0864(9)	0.013(2)	12(2)
C(2)	0.167(1)	0.155(1)	0.093(2)	14(3)
C(3)	0.2111(9)	0.138(1)	0.007(1)	11(2)
C(4)	0.1295(8)	0.0948(9)	0.473(1)	9(1)
C(5)	0.169(1)	0.1619(9)	0.394(2)	11(2)
C(6)	0.2089(9)	0.142(1)	0.482(2)	11(2)
C(7)	0.0400(9)	–0.053(1)	0.329(2)	14(2)
C(8)	0.060(1)	–0.096(1)	0.243(2)	15(2)
C(9)	0.0355(9)	–0.050(1)	0.178(2)	14(2)
N	0.3266(6)	0.0790(6)	0.084(1)	5.7(9)
C(10)	0.3269(8)	0.1079(8)	0.145(2)	7(1)
C(11)	0.3209(9)	0.0917(9)	0.213(2)	8(1)
C(12)	0.3268(9)	0.1246(9)	0.263(2)	8(1)
C(13)	0.321(1)	0.111(1)	0.336(2)	12(2)
C(14)	0.3328(9)	0.0982(8)	0.010(2)	8(1)
C(15)	0.2991(9)	0.1020(8)	–0.017(2)	8(1)
C(16)	0.314(2)	0.121(1)	–0.088(2)	15(3)
C(17)	0.278(1)	0.126(1)	–0.117(2)	12(2)
C(18)	0.2880(8)	0.0417(8)	0.090(2)	7(1)
C(19)	0.284(1)	0.0133(9)	0.032(2)	10(2)
C(20)	0.241(1)	–0.0195(9)	0.031(2)	9(2)
C(21)	0.2293(9)	–0.041(1)	0.100(2)	9(2)
C(22)	0.358(1)	0.069(1)	0.098(2)	10(2)
C(23)	0.398(1)	0.102(1)	0.096(3)	15(2)
C(24)	0.435(2)	0.099(2)	0.089(3)	16(4)*
C(25)	0.429(2)	0.080(2)	0.160(3)	12(2)*
C(24)′	0.426(2)	0.088(2)	0.108(5)	5(3)*
C(25)′	0.466(2)	0.115(3)	0.139(6)	13(5)*
P(4)	0.0643(5)	0.4399(6)	0.0338(9)	8.4(7)*
C(26)	0.0141(9)	0.409(2)	0.051(4)	18(4)*
C(27)	0.084(2)	0.409(2)	0.035(3)	12(2)*
C(28)	0.066(2)	0.453(2)	–0.056(2)	11(2)*
P(4)′	0.0595(8)	0.4124(9)	0.036(1)	11(1)*
C(26)′	0.025(2)	0.423(2)	0.074(3)	9(2)*
C(27)′	0.097(1)	0.426(2)	0.099(3)	11(3)*
C(28)′	0.081(2)	0.445(3)	–0.035(3)	33(9)*
B	0.3421(6)	0.3580(6)	0.102(1)	15(2)*
F(1)	0.3031(6)	0.340(1)	0.111(2)	11(2)*
F(2)	0.351(1)	0.3751(9)	0.038(1)	11(2)*
F(3)	0.362(1)	0.384(1)	0.153(2)	17(2)*
F(4)	0.353(1)	0.330(1)	0.102(2)	15(2)*
F(1)′	0.316(1)	0.369(1)	0.086(2)	13(2)*
F(2)′	0.344(1)	0.356(1)	0.175(1)	14(2)*
F(3)′	0.3768(9)	0.386(1)	0.078(3)	24(3)*
F(4)′	0.332(1)	0.3235(8)	0.075(2)	17(2)*
O	0.051(1)	0.5188(9)	0.049(2)	10(1)*
C(29)	0.077(1)	0.557(1)	0.015(2)	8(2)*
C(30)	0.074(2)	0.5879(9)	0.057(3)	9(2)*
C(31)	0.049(2)	0.569(2)	0.122(3)	12(2)*
C(32)	0.034(2)	0.526(1)	0.116(3)	12(2)*

[a] Starred values indicate that atoms were refined isotropically. Anisotropically refined atoms are given in the form of the equivalent isotropic displacement parameter defined as $(4/3)[a^2\beta_{11} + b^2\beta_{22} + c^2\beta_{33} + ab(\cos\gamma)\beta_{12} + ac(\cos\beta)\beta_{13} + bc(\cos\alpha)\beta_{23}]$.

Table VII. Selected Bond Distances (Å) and Angles (deg) for $(HPMe_3)(Bu_4N)[Nb_3Cl_{10}(PMe_3)_3](BF_4)\cdot THF$[a]

Distances

Nb(1)–Nb(2)	2.974(3)	Nb(2)–Cl(3)	2.452(6)
Nb(1)–Nb(3)	2.944(3)	Nb(2)–Cl(7)	2.418(5)
Nb(1)–Cl(1)	2.500(7)	Nb(2)–Cl(8)	2.408(8)
Nb(1)–Cl(2)	2.456(8)	Nb(2)–P(2)	2.650(9)
Nb(1)–Cl(4)	2.446(5)	Nb(3)–Cl(1)	2.494(5)
Nb(1)–Cl(5)	2.406(8)	Nb(3)–Cl(3)	2.468(8)
Nb(1)–Cl(6)	2.414(5)	Nb(3)–Cl(4)	2.436(7)
Nb(1)–P(1)	2.638(9)	Nb(3)–Cl(9)	2.419(8)
Nb(2)–Nb(3)	2.958(3)	Nb(3)–Cl(10)	2.415(9)
Nb(2)–Cl(1)	2.493(8)	Nb(3)–P(3)	2.636(6)
Nb(2)–Cl(2)	2.459(8)		

Angles

Nb(2)–Nb(1)–Nb(3)	59.99(6)	Cl(3)–Nb(2)–Cl(8)	90.0(2)
Cl(1)–Nb(1)–Cl(2)	105.7(2)	Cl(3)–Nb(2)–P(2)	83.1(2)
Cl(1)–Nb(1)–Cl(4)	106.1(2)	Cl(7)–Nb(2)–Cl(8)	90.5(2)
Cl(1)–Nb(1)–Cl(5)	88.6(3)	Cl(7)–Nb(2)–P(2)	81.4(2)
Cl(1)–Nb(1)–Cl(6)	88.2(2)	Cl(8)–Nb(2)–P(2)	81.5(3)
Cl(1)–Nb(1)–P(1)	166.6(3)	Nb(1)–Nb(3)–Nb(2)	60.51(6)
Cl(2)–Nb(1)–Cl(4)	87.1(2)	Cl(1)–Nb(3)–Cl(3)	105.9(2)
Cl(2)–Nb(1)–Cl(5)	165.7(3)	Cl(1)–Nb(3)–Cl(4)	106.6(2)
Cl(2)–Nb(1)–Cl(6)	90.3(2)	Cl(1)–Nb(3)–Cl(9)	88.7(2)
Cl(2)–Nb(1)–P(1)	84.2(3)	Cl(1)–Nb(3)–Cl(10)	88.1(2)
Cl(4)–Nb(1)–Cl(5)	90.0(2)	Cl(1)–Nb(3)–P(3)	166.9(3)
Cl(4)–Nb(1)–Cl(6)	165.6(3)	Cl(3)–Nb(3)–Cl(4)	87.1(3)
Cl(4)–Nb(1)–P(1)	83.0(2)	Cl(3)–Nb(3)–Cl(9)	90.2(3)
Cl(5)–Nb(1)–Cl(6)	89.1(2)	Cl(3)–Nb(3)–Cl(10)	165.8(2)
Cl(5)–Nb(1)–P(1)	81.5(3)	Cl(3)–Nb(3)–P(3)	83.3(2)
Cl(6)–Nb(1)–P(1)	82.7(2)	Cl(4)–Nb(3)–Cl(9)	164.6(2)
Nb(1)–Nb(2)–Nb(3)	59.50(6)	Cl(4)–Nb(3)–Cl(10)	90.9(3)
Cl(1)–Nb(2)–Cl(2)	105.8(2)	Cl(4)–Nb(3)–P(3)	82.7(2)
Cl(1)–Nb(2)–Cl(3)	106.5(2)	Cl(9)–Nb(3)–Cl(10)	88.0(3)
Cl(1)–Nb(2)–Cl(7)	89.2(2)	Cl(9)–Nb(3)–P(3)	81.9(3)
Cl(1)–Nb(2)–Cl(8)	88.1(3)	Cl(10)–Nb(3)–P(3)	82.5(3)
Cl(1)–Nb(2)–P(2)	166.0(3)	Nb(1)–Cl(1)–Nb(2)	73.1(2)
Cl(2)–Nb(2)–Cl(3)	86.6(2)	Nb(1)–Cl(1)–Nb(3)	72.2(2)
Cl(2)–Nb(2)–Cl(7)	89.2(2)	Nb(2)–Cl(1)–Nb(3)	72.8(2)
Cl(2)–Nb(2)–Cl(8)	166.1(3)	Nb(1)–Cl(2)–Nb(2)	74.5(3)
Cl(2)–Nb(2)–P(2)	84.7(3)	Nb(2)–Cl(3)–Nb(3)	73.9(2)
Cl(3)–Nb(2)–Cl(7)	164.3(3)	Nb(1)–Cl(4)–Nb(3)	74.2(2)

[a] Numbers in parentheses are estimated standard deviations in the least significant digits.

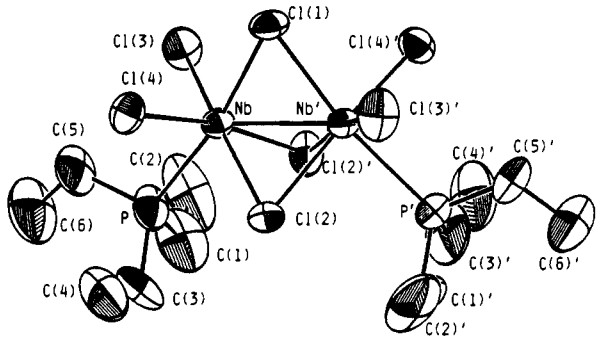

Figure 2. Configuration of $[Nb_2Cl_7(PEt_3)_2]^-$ showing the atom-labeling scheme. Thermal ellipsoids are presented at the 50% probability level.

are longer than the Nb–Cl bonds (2.403(5)–2.524(5) Å), a trans influence of the phosphine ligands is still observable, since the bond distances for Nb–$Cl_{bridging}$ bonds trans to phosphorus atoms and trans to terminal chlorine atoms are 2.524(5) and 2.498[8] Å, respectively. The average Nb–$Cl_{bridging}$ distance, 2.502[17] Å, is a little longer than that of the Nb–$Cl_{terminal}$ bonds, 2.403(5) Å, which is common in face-sharing bioctahedral transition metal clusters.[25]

Finally, the average Nb–$Cl_{bridging}$–Nb angle 65.5[4]° is 5.0° less than that of an ideal face-sharing bioctahedral structure

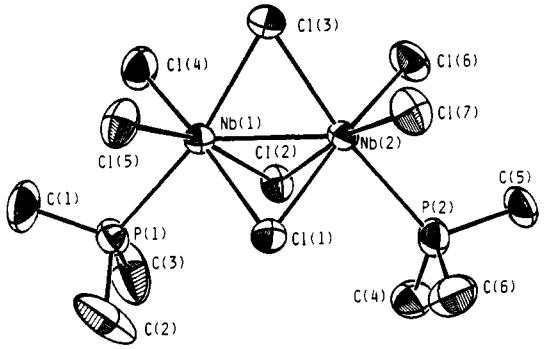

Figure 3. Configuration of $[Nb_2Cl_7(PMe_3)_2]^-$ showing the atom-labeling scheme. Thermal ellipsoids are presented at the 50% probability level.

Table VIII. Comparison of Some Important Bond Parameters for **1** and **2**[a]

	1	2
Nb–Nb, Å	2.708(3)	2.683(1)
Nb–$Cl_{bridging}$, Å		
trans to P	2.524(5)	2.538[4]
cis to P	2.494[8]	2.490[6]
average	2.502[17]	2.506[23]
Nb–$Cl_{terminal}$, Å	2.403(5)	2.404[12]
Nb–P, Å	2.617(6)	2.584[7]
Nb–$Cl_{bridging}$–Nb, deg	65.4[4]	64.7[7]

[a] Square brackets denote mean deviation from the unweighted arithmetic mean.

(70.5°), which is indicative of a compression effect caused by a metal–metal bonding interaction.

Crystal Structure of $(Bu_4N)[Nb_2Cl_7(PMe_3)_2]\cdot THF$ (2). The crystal structure of the trimethylphosphine derivative is composed of tetrabutylammonium cations, diniobium cluster anions, and interstitial tetrahydrofuran solvent molecules. The configuration of the diniobium cluster anion is shown in Figure 3. This is the same type of structure as that seen in the above triethylphosphine derivative. Although there is no crystallographic symmetry element passing through the cluster anion, it also possesses effectively a C_{2v} symmetry for the skeletal structure. The metal–metal distance 2.683(1) Å is only 0.02 Å shorter than the one in its PEt_3 analogue, and the differences between other important bonding parameters are essentially within the 3σ criterion, as can be seen from the comparison made in Table VIII.

It is interesting to note that these two metal–metal distances are well within the narrow range, 2.684(1)–2.728(5) Å, spanned by all known face-sharing bioctahedral diniobium(III) clusters (Table IX) except perhaps for $Cs_3Nb_2Br_9$ and $Cs_3Nb_2I_9$ where the larger halogen atoms probably cause real increases although the large esd's (2.77(3) and 2.96(9) Å, respectively)[26] make exact comparison difficult. This is in sharp contrast to the situation for their dimolybdenum(III) analogues, where the metal–metal distances drop considerably from ca. 2.7 Å for halide-only-bridged ones to ca. 2.4 Å for halide-sulfide-bridged ones.[32]

Crystal Structure of $(HPMe_3)(Bu_4N)[Nb_3Cl_{10}(PMe_3)_3](BF_4)\cdot THF$ (3). The crystal structure determination has revealed an unusual combination of ions and solvents: the triangular

(25) Cotton, F. A.; Walton, R. A. *Multiple Bonds between Metal-Metal Atoms*, 2nd ed.; Oxford Press: Oxford, U.K., 1993.

(26) Broll, A.; Von Schnering, H. G.; Schafer, H. *J. Less-Common Met.* **1970**, *22*, 243.

(27) Cotton, F. A.; Najjar, R. C. *Inorg. Chem.* **1981**, *20*, 2716.

(28) Templeton, J. L.; Dorman, W. C.; Clardy, J. C.; McCarley, R. E. *Inorg. Chem.* **1978**, *17*, 1263.

(29) Cotton, F. A.; Duraj, S. A.; Roth, W. J. *Acta Crystallogr.* **1985**, *C41*, 878.

(30) Cotton, F. A.; Falvello, L. R.; Najjar, R. C. *Inorg. Chim. Acta* **1982**, *63*, 107.

(31) Gilletti, P. E.; Young, V. G.; Brown, T. M. *Inorg. Chem.* **1989**, *28*, 4034.

(32) (a) Moynihan, K. J.; Gao, X.; Boorman, P. M.; Fait, J. F.; Freeman, G. K. W.; Thornton, P.; Ironmonger, D. J. *Inorg. Chem.* **1990**, *29*, 1648. (b) Boorman, P. M.; Moynihan, K. J.; Oakley, R. T. *J. Chem. Soc., Chem. Commun.* **1982**, 899.

Table IX. Important Bond Distances (Å) of Face-Sharing Bioctahedral Diniobium(III) and Ditantalum(III) Compounds

	M–M	M–X_b[a]	M–S_b[b]	M–X_t[c]	M–L_t[d]	ref
$Cs_3Nb_2Cl_9$	2.70(1)					26
$Ta_2Cl_6(THT)_3$	2.681(1)	2.503[9]	2.390[1]	2.366[4]	$2.629[7]_S$	27
$Ta_2Br_6(THT)_3$	2.710(2)	2.633[10]	2.393[3]	2.516[3]	$2.624[3]_S$	28
$Nb_2Br_6(THT)_3$	2.728(5)	2.626[10]	2.487[32]	2.534[6]	$2.632[41]_S$	28
$Ta_2Cl_6(SMe_2)_3$	2.691(1)	2.499[21]	2.378(5)	2.372[7]	$2.618(5)_S$	27
$Ta_2Cl_6(SMe_2)(THF)_2$	2.6695(5)	2.494[1]	2.370[1]	2.368[1]	$2.229[10]_O$	29
$Nb_2Cl_6(SMe_2)(THF)_2$	2.684(2)	2.489[2]	2.406[1]	2.375[5]	$2.234[1]_O$	29
$Ta_2Cl_6(SMe_2)[(Me_2N)_3P]_2$	2.704(1)	2.500[7]	2.400[3]	2.347[3]	$2.726[3]_P$	30
$[Ta_2Cl_6(THT)]_2(dppe)_2$	2.704(2)	2.495[15]	2.395[7]	2.369[6]	$2.753[7]_P$	31

[a] X_b denotes bridging halide. [b] S_b denotes bridging sulfide. [c] X_t denotes terminal halide. [d] L_t denotes terminal ligand.

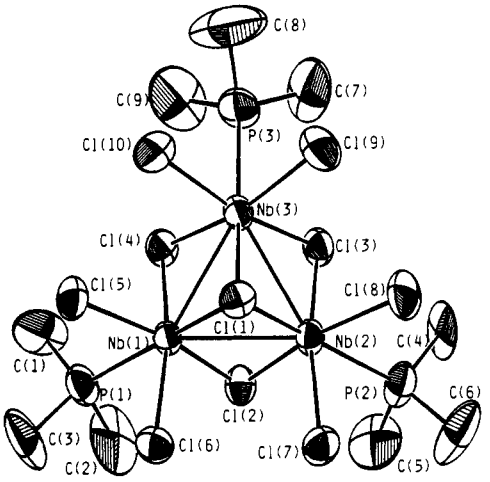

Figure 4. Configuration of $[Nb_3Cl_{10}(PMe_3)_3]^-$ showing the atom-labeling scheme. Thermal ellipsoids are presented at the 50% probability level.

trinuclear niobium cluster anions cocrystallize with trimethylphosphonium and tetrabutylammonium cations, tetrafluoroborate anions, and interstitial tetrahydrofuran solvent molecules in a 1:1:1:1:1 ratio. The trinuclear niobium cluster anion is shown in Figure 4. The triangle of three niobium atoms is capped by a chlorine atom and the edges are bridged by three chlorine atoms to form a cubane-like framework that is missing one apex. Each niobium is further coordinated terminally by two chlorine atoms and a trimethylphosphine ligand to complete a common M_3X_{13} type structure.[33] So far all the known $[Nb_3Cl_{10}(PR_3)_3]^-$ clusters adopt this type structure and have approximately C_{3v} symmetry. The metal–metal distances are 2.974(3), 2.944(3), and 2.958(3) Å; the average value of 2.959[12] Å falls at the lower end of the narrow range, 2.960[3]–2.976[8] Å, for those reported so far. The other bonding parameters are all comparable to those previously reported, as shown in Table X. For comparison, parameters are also listed for the cluster $Nb_3Cl_7(PMe_2Ph)_6$, which is the only one with eight cluster core electrons. This has an appreciably shorter metal–metal distance, 2.834[4] Å, which implies bonding character for the two extra electrons.

Formation of Nb_2 and Nb_3 Cluster Compounds. In our previous reports on the synthesis of niobium and tantalum trinuclear clusters,[2] we have pointed out that the reactions are generally not clean and the yields are low. We have tried different ways to improve the yields, such as addition of $MgCl_2$ or tetraalkylammonium chloride to provide enough $[Mg_2Cl_3(THF)_6]^+$ or other counterions, and use of different kinds of reducing agents and combinations of solvents, but without great effect. Along with the trinuclear clusters there were always large quantities of precipitates or oily substances formed. In the niobium case, we have found consistently that the first step in the reduction of $NbCl_4(THF)_2$ results in a green substance. Sometimes this is transient, as in the reduction in toluene by Na/Hg to synthesize $Nb_3Cl_7(PMe_2Ph)_6$ and $(HPEt_3)[Nb_3Cl_{10}(PEt_3)_3]$.[1] In some other cases, the green precipitate persisted, was filtered off and redissolved leading to the isolation of trinuclear products. This occurred during the preparations of $[Mg_2Cl_3(THF)_6][Nb_3Cl_{10}(PEt_3)_3]$ and $(HPEt_3)[Nb_3Cl_{10}(PEt_3)_3]$ by reduction in THF by Mg.[2] The most persistent green substance was obtained in the reduction of $NbCl_4(THF)_2$ in THF by Na/Hg with no phosphine present. In this case the green precipitate was virtually insoluble and had to be removed by filtration in order to allow the isolation of a small amount of $Na[Nb_3Cl_{10}(THF)_3]$ from the filtrate.[2]

In the beginning of reduction of $NbCl_4(THF)_2$ by Mg in THF in the presence of PEt_3, a weak band at 435 nm is seen along with the very intense dimer band at 637 nm (Figure 1a). This weak band is at the same position as the trimer band, as shown by the measurements on authentic samples of $(HPEt_3)[Nb_3Cl_{10}(PEt_3)_3]$ and $[Mg_2Cl_3(THF)_6][Nb_3Cl_{10}(PEt_3)_3]$, and is thus indicative of the formation of the trinuclear cluster $[Nb_3Cl_{10}(PEt_3)_3]^-$. As the reaction proceeds, the intensity of the band at 435 nm increases, while that of the dimer band at 637 nm decreases (Figure 1b), which indicates that the reaction entails transformation of a dinuclear cluster into a trinuclear one. Under ambient conditions, the dimer band will disappear in about a week (Figure 1d). The tracking experiments have also shown that the addition of $MgCl_2$ or Bu_4NBF_4, like an increase in the temperature, can accelerate the formation of trimers, which may be understandable from the point of view of providing additional counterions, such as $[Mg_2Cl_3(THF)_6]^+$ and Bu_4N^+, as required by the stoichiometry, as discussed previously.[2]

Incomplete conversion of dinuclear clusters to the corresponding trinuclear ones may constitute one of the major factors that diminish yields for trimers. In a typical case, the yield for $Na[Nb_3Cl_{10}(THF)_3]$ is only 15%, since its probable dimer precursor, $[Nb_2Cl_7(THF)_nCl_{2-n}]^{-3+n}$, (vide infra) has a very low solubility which impedes good conversion. There may be a similar situation in the preparative reaction for $[Nb_3Cl_{10}(PMe_3)_3]^-$, the yield being only 11%. However, in the preparation of the trimer anion $[Nb_3Cl_{10}(PEt_3)_3]^-$, the dimer precursor $[Nb_2Cl_7(PEt_3)_2]^-$ has a much better solubility and the yield is generally 30%.[1]

The tracking experiments have shown that the accumulation of the trimer in solution is limited. After 3 days of stirring a brown, intractable precipitate is formed, which contributes to the rising background in the visible spectrum. Eventually, along with the accumulation of the brown precipitate, the dimer disappears and the trimer concentration in solution also decreases. We do not know yet the structure of the brown precipitate, but the formation of clusters with higher nuclearities such as $Nb_4Cl_{10}(PR_3)_6$[3] under similar reaction conditions as well as the insolubility of the precipitate in common organic solvents, make it highly possible that the precipitate consists of one or more oligomers with higher nuclearities. Thus, the formation of the trimer may not be the final stage of the reaction, and the conversion of trimers to other clusters with higher nuclearity may be one of the major factors that diminish the yield for the trimer. In hindsight, it can be understood why we obtained a relatively good yield of the trimer $(HPEt_3)[Nb_3Cl_{10}(PEt_3)_3]$.[2] In this procedure we caused the reaction to stop at an early stage of dimer-to-trimer transformation by depositing the dimer-trimer mixture with

(33) Muller, A.; Jostes, R.; Cotton, F. A. *Angew. Chem., Int. Ed. Engl.* **1980**, *19*, 875.

Table X. Important Bond Distances for Nb and Ta Trimers Containing Only Phosphine and Halide Ligands

	M–M	M–P	M–Cl_c[a]	M–Cl_b[b]	M–Cl_t[c]	ref
$(HPMe_3)(Bu_4N)[Nb_3Cl_{10}(PMe_3)_3](BF_4)\cdot THF$	2.959[12]	2.641[6]	2.496[3]	2.453[10]	2.413[5]	this work
$(HPEt_3)[Nb_3Cl_{10}(PEt_3)_3]$	2.970[6]	2.656[9]	2.500[13]	2.438[5]	2.416[16]	2
$(HPEt_3)[Nb_3Cl_{10}(PEt_3)_3]\cdot 1.25C_7H_8$	2.976[8]	2.667[4]	2.504[1]	2.443[8]	2.424[8]	1
$[Mg_2Cl_3(THF)_6][Nb_3Cl_{10}(PEt_3)_3]\cdot 2THF$	2.954[6]	2.666[28]	2.498[6]	2.451[11]	2.403[7]	2
$[Mg_2Cl_3(THF)_6][Nb_3Cl_{10}(PMe_2Ph)_3]\cdot 2THF$	2.960[3]	2.654[4]	2.497[7]	2.438[13]	2.419[6]	2
$(HPEt_3)[Ta_3Cl_{10}(PEt_3)_3]$	2.932[4]	2.649[2]	2.499[9]	2.431[4]	2.416[8]	1
$Nb_3Cl_7(PMe_2Ph)_6$	2.832[4]	2.696[2][d]	2.470[5]	2.476[3][e]	2.485[6]	1
		2.731[8][f]		2.531[4][g]		

[a] Cl_c denotes capping chloride. [b] Cl_b denotes bridging chloride. [c] Cl_t denotes terminal chloride. [d] Trans to Cl_b. [e] Trans to Cl_t. [f] Trans to Cl_c. [g] Trans to P.

Table XI. Magnetic Susceptibility Data for Face-Sharing Bioctahedral Diniobium(III) and Ditantalum(III) Cluster Compounds[a]

	$10^6\chi_{app}$, emu/g	$10^6\chi_M$, emu/mol	$10^6\chi_{cor}$, emu/mol	μ_{eff}, μ_B	T, K	ref
$Cs_3Nb_2I_9$[b]				2.74		26
$Cs_3Nb_2Br_9$[b]				2.68		26
$(Et_4N)_3Nb_2Cl_9$	0.464	416	1024	1.56	297	35
$(Bu_4N)[Nb_2Cl_7(PMe_3)_2]\cdot THF$	–0.09	–78	411	0.99	299	this work
$(Bu_4N)[Nb_2Cl_7(PEt_3)_2]$	–0.29	–266	294	0.84	299	this work
$Nb_2Cl_6(THT)_3$	–0.282	–187	193	0.67	295	35
$Ta_2Br_6(THT)_3$	–0.24	–254	177	0.65	298	28
$(Et_4N)_2[Nb_2Cl_8(THT)]$	–0.408	–334	198	0.51	297	35
$Ta_2Cl_6(THT)_3$	–0.33	–276	95	0.48	298	28

[a] χ_{app} = apparent susceptibility per gram; χ_M = molar susceptibility; χ_{cor} = susceptibility corrected for diamagnetic susceptibility per mole. [b] These two compounds were apparently measured over the temperature range 200–500 K. They were also said to have very large Weiss constants, –210 K (Br) and –370 K (I). No magnetic data were given for $Cs_3Nb_2Cl_9$.

hexane and then redissolved the mixture in THF and layered the solution with hexane.[2] The trimer produced in situ was thus separated promptly from the reaction system by crystallization due to a reduced solubility in the THF/hexane solvent mixture.

Another point of note in our tracking experiments is that after the reduction by Mg, there is a band discernible at 490 nm (Figure 1a), although it is very weak. As the reaction proceeds, the intensity diminishes (Figure 1b) and eventually it disappears (Figure 1c). It has been well documented that edge-sharing bioctahedral niobium dimers $Nb_2Cl_6(R_2PR'PR_2)_2$ ($R_2PR'PR_2$ denotes bidentate phosphines, such as depe, dppm, dppe, and dmpm.) are generally purple in solution. Since a band at 490 nm is consistent with a purple color, it seems reasonable that the purple compound existing in the early stage of the reaction may be an edge-sharing bioctahedral complex with monodentate phosphine, viz., $Nb_2Cl_6(PEt_3)_4$.

The earlier observations just cited as well as the reaction tracking experiments reported here show (a) that in all preparations of trinuclear niobium clusters by reduction of $NbCl_4(THF)_2$ there is a green intermediate and (b) that a solution of this type of green intermediate in the presence of phosphines has an intense absorption band at 637 nm. We have now found the conditions that enable us to isolate, from such green solutions, crystalline solids, and we find that the species responsible for the green color are the $[Nb_2Cl_7(PR_3)_2]^-$ ions. When an isolated salt of a $[Nb_2Cl_7(PR_3)_2]^-$ ion is redissolved in THF, the solution again shows the 637 nm band. Moreover, in other noncoordinating solvents, such as benzene and dichloromethane, solutions of $[Nb_2Cl_7(PR_3)_2]^-$ are also green, which is further evidence that the dimer form found in the solid state can well be retained in the solution phase. Although we have not been able to explicitly identify the green substance obtained in reduction by Mg in THF with no phosphine present, it is reasonable to assume it to be $[Nb_2Cl_7(THF)_nCl_{2-n}]^{-3+n}$ (n = 1 or 2), an analogue with phosphines replaced by THF and chloride, based on the similarity to the reaction in the presence of a phosphine.

We believe that by firmly establishing that $[(R_3P)Cl_2Nb(\mu\text{-}Cl)_3NbCl_2(PR_3)]^-$ species exist and that they are often, if not always, responsible for the green colors that proceed the formation of trinuclear species of the type $[Nb_3(\mu_3\text{-}Cl)(\mu\text{-}Cl)_3Cl_n(PR_3)_{9-n}]^{5-n}$, we are now in a position to consider some ways in which trinuclear and tetranuclear products might be formed.

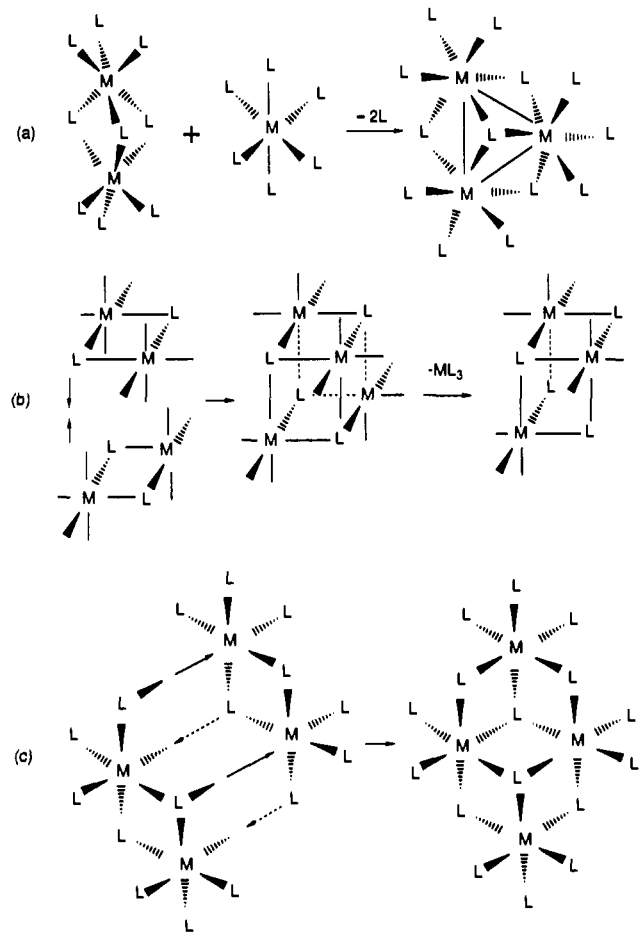

Figure 5. Conversion of the Nb_2 to the Nb_3 cluster.

We now propose that in the formation of all trinuclear (and higher order) clusters, dinuclear clusters are necessary intermediates. These dinuclear intermediates may be the type of face-sharing species with three chlorine bridges that we have

characterized in detail or they might be edge-sharing species that appear transiently but do not accumulate the way the green face-sharing species do. In any event, from the face-sharing binuclear stage one may imagine two general ways to obtain a trinuclear species. One is by the attachment of some transient mononuclear species to the dinuclear species, for example as shown schematically in Figure 5a. It is then possible that by further additions of this kind tetranuclear clusters as well as still larger ones could be built up.

On the other hand, we might also consider the possibility that two dinuclear species could be combined to form a tetramer, for example as shown in Figure 5b, and that trinuclear species might then arise by loss of one metal atom from this tetranuclear species. This is known to be the way in which some $Mo_3S_4L_9$ type clusters are formed.[34]

Still another possibility is that two dinuclear species might approach each other and form a rhomboidal tetranuclear species, as in Figure 5c. Molecules such as this could persist and be isolable under some circumstances[3] or, as in the previous case, extrude one metal atom to leave the trinuclear cluster.

It will be difficult, and might not even be possible, to prove or disprove the occurrence of these pathways, but we believe that they represent credible possibilities, given that face-sharing binuclear species have been shown to be isolable precursors to trinuclear and higher-order clusters.

Magnetic Properties of Face-Sharing Bioctahedral Diniobium(III) and Ditantalum(III) Clusters. The magnetic susceptibility data for **1** and **2** at room temperature are listed in Table XI along with such data for other face-sharing bioctahedral diniobium(III) and ditantalum(III) species. The magnetic moments decrease from cesium nonahalide salts to the tetraalkylammonium salt, and to clusters with terminal phosphines, and finally to clusters with one bridging halide replaced by a thioether ligand.

At present our understanding of these magnetic properties is very limited and very tentative. In the original report[26] of the two Cs salts it was suggested that there are two unpaired electrons, but the very large Weiss constants make a simple interpretation doubtful. It is true that in the D_{3h} symmetry of these $[Nb_2Cl_9]^{3-}$ ions one might well expect $\sigma^2\pi^2$ configurations so that at higher temperatures two unpaired π bonding electrons would give rise to a magnetic moment of the order of those reported. However, the lower value reported[35] for $(Et_4N)_3[Nb_2Cl_9]$ is not easily reconciled with the same expectation, and Maas and McCarley suggested that in this case, as in all the THT compounds[28,35] the weak paramagnetism is of the Van Vleck temperature-independent type. For the THT compounds the symmetry is lowered to C_{2v} and the degeneracy of the two π orbitals is lifted.[28] Thus, the absence of unpaired electrons could be rationalized in these cases. This is not possible, however, for the $[Nb_2Cl_9]^{3-}$ ion where D_{3h} symmetry is still present, so far as is known. The properties of the $[Nb_2Cl_9]^{3-}$ ion are currently under further investigation by us.

It is true that the two $[Nb_2Cl_7(PR_3)_2]^-$ ions have symmetry C_{2v} and could thus also have no unpaired electrons, but the central bridging unit, $Nb(\mu\text{-}Cl)_3Nb$, deviates little from D_{3h} symmetry. Again, however, the susceptibilities are low and correspond to magnetic moments far below expectation for two unpaired electrons. We do not yet know whether the susceptibilities of these species are temperature-dependent or not.

Acknowledgment. We thank the Robert A. Welch Foundation for support under Grant No. A494.

Supplementary Material Available: Full tables of crystallographic data, listings of anisotropic thermal parameters, and full tables of bond distances and angles for the crystal structures of **1–3**, ORTEP drawings of unit cell contents for **1** and **2**, and disorder models for **3** (27 pages). Ordering information is given on any current masthead page.

(34) Martinez, M.; Ooi, B.-L.; Sykes, A. G. *J. Am. Chem. Soc.* **1987**, *109*, 4615.

(35) Maas, E. T., Jr.; McCarley, R. E. *Inorg. Chem.* **1973**, *12*, 1096.